Jets 2021 Conference

Black Hole Spin Determinations for over 750 Sources

Ruth A Daly

Details are presented in Daly (2016; 2019; 2021) &
Daly, Stout [undergrad], & Mysliwiec [undergrad] (2018)
More information is available at https://sites.psu.edu/rdaly/

Overview

Astrophysical Black Holes (BH) are characterized by their mass and spin.
To date there are precious few methods to measure spin values
=> **it is important to develop new methods to measure BH spin values.**

$\Rightarrow$ **new method, the "Outflow Method," proposed & developed by D16, D+18, D19, & D21 (+ D09a,b; D11).**

$\Rightarrow$ **Four samples: 100 FRII sources; 576 LINERS; 80 Local AGN; 102 measurements of 4 stellar mass BH**

Key empirically determined ingredients:

L_j = outflow beam power, dE/dt (in kinetic energy), (strong shock method & the fundamental line mapping method)
L_{bol} = accretion disk bolometric luminosity, (from [OIII] and (2-10) keV luminosities)
L_{Edd} = black hole mass (i.e. Eddington luminosity), (Obtained with standard, well-accepted techniques)

These quantities are combined to obtain BH spin, accretion disk magnetic field strength, + other properties.

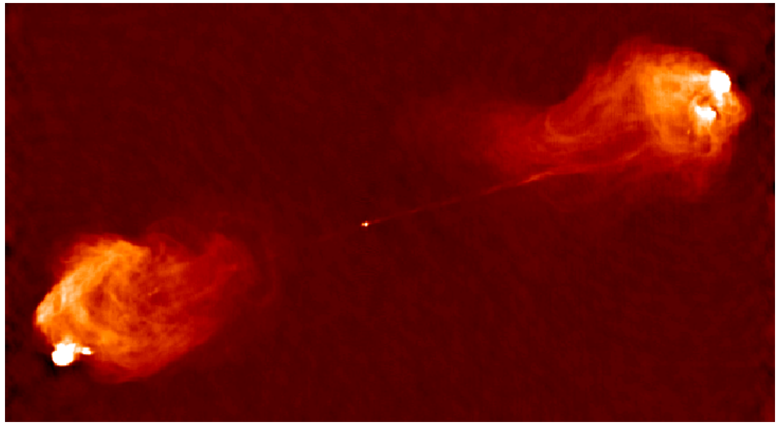

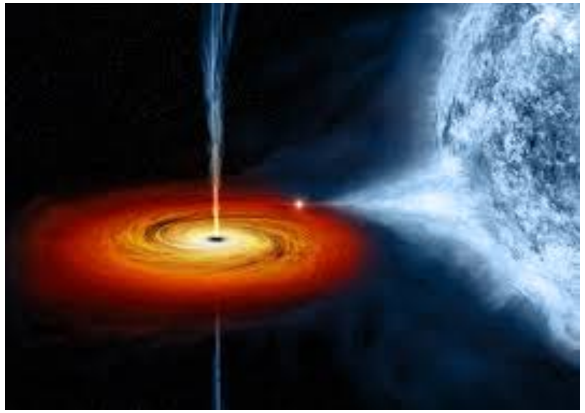

BH Systems with Disk and Outflow Activity (D+18)
=> All governed by the same physical processes

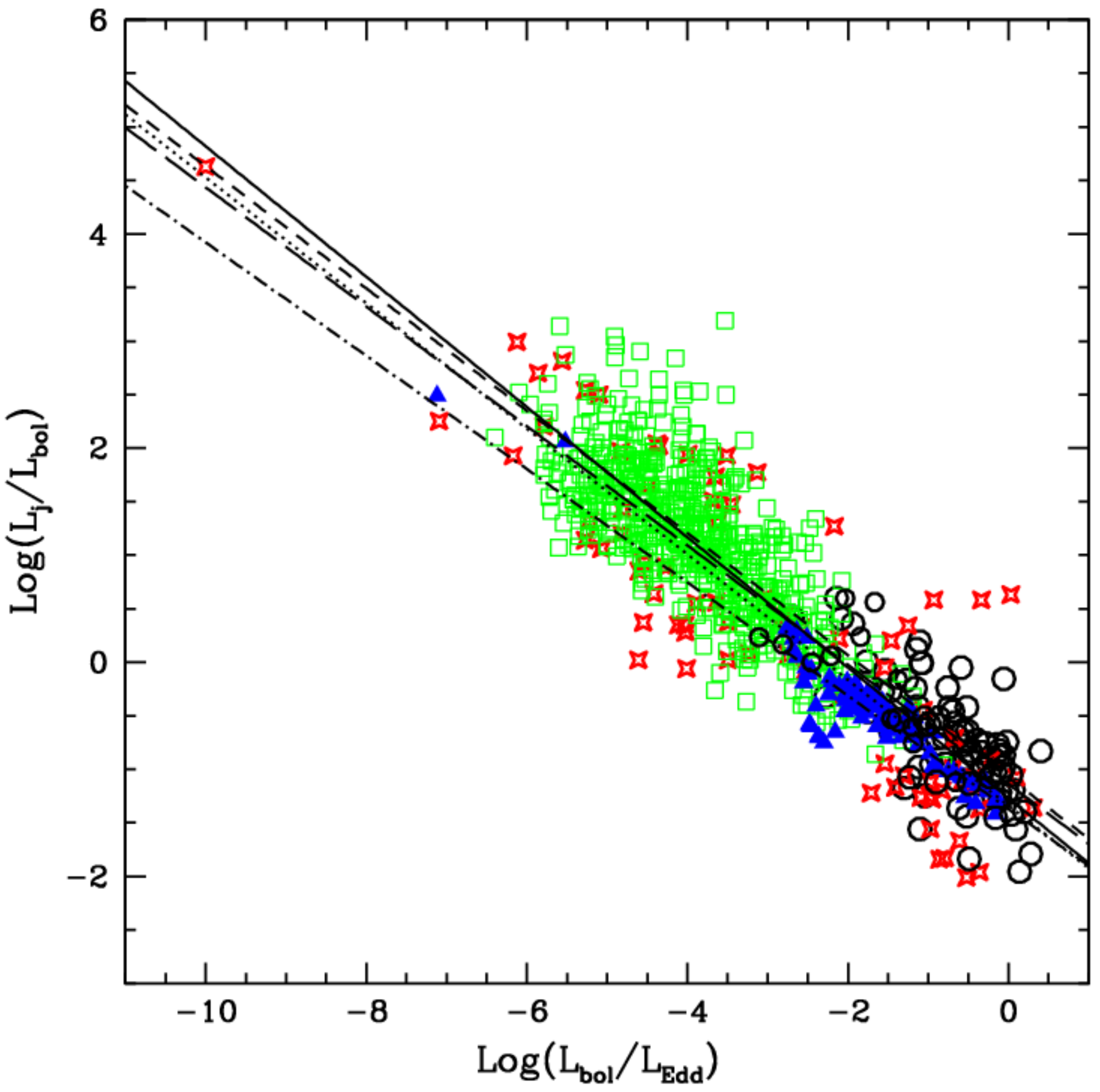

4 Categories of BH considered (D+18):

3 types of supermassive BH +
1 type of stellar-mass BH

100 FRII sources - shown in black (D16)
576 LINERs (Nisbet & Best 2016) – shown in green
80 AGN (Merloni et al. 2003) – shown in red
102 (of 4) Stellar-mass Galactic black holes – shown in blue (Saikia et al. 2015)

Best fit slopes (A-1):

-0.56 ± 0.05 for 100 FRII sources (long-dashed line)
-0.57 ± 0.02 for 576 LINERs (med-dashed line)
-0.59 ± 0.04 for 80 Compact RS AGN (dotted line)
-0.53 ± 0.02 for 102 GBH (dot-dashed line)
The solid line shows the fit to all sources (from D+18)

$(L_j/L_{bol}) \propto (L_{bol}/L_{EDD})^{A-1}$ **Strictly empirical**

BH Systems with Disk and Outflow Activity (D+18)
=> All governed by the same physical processes

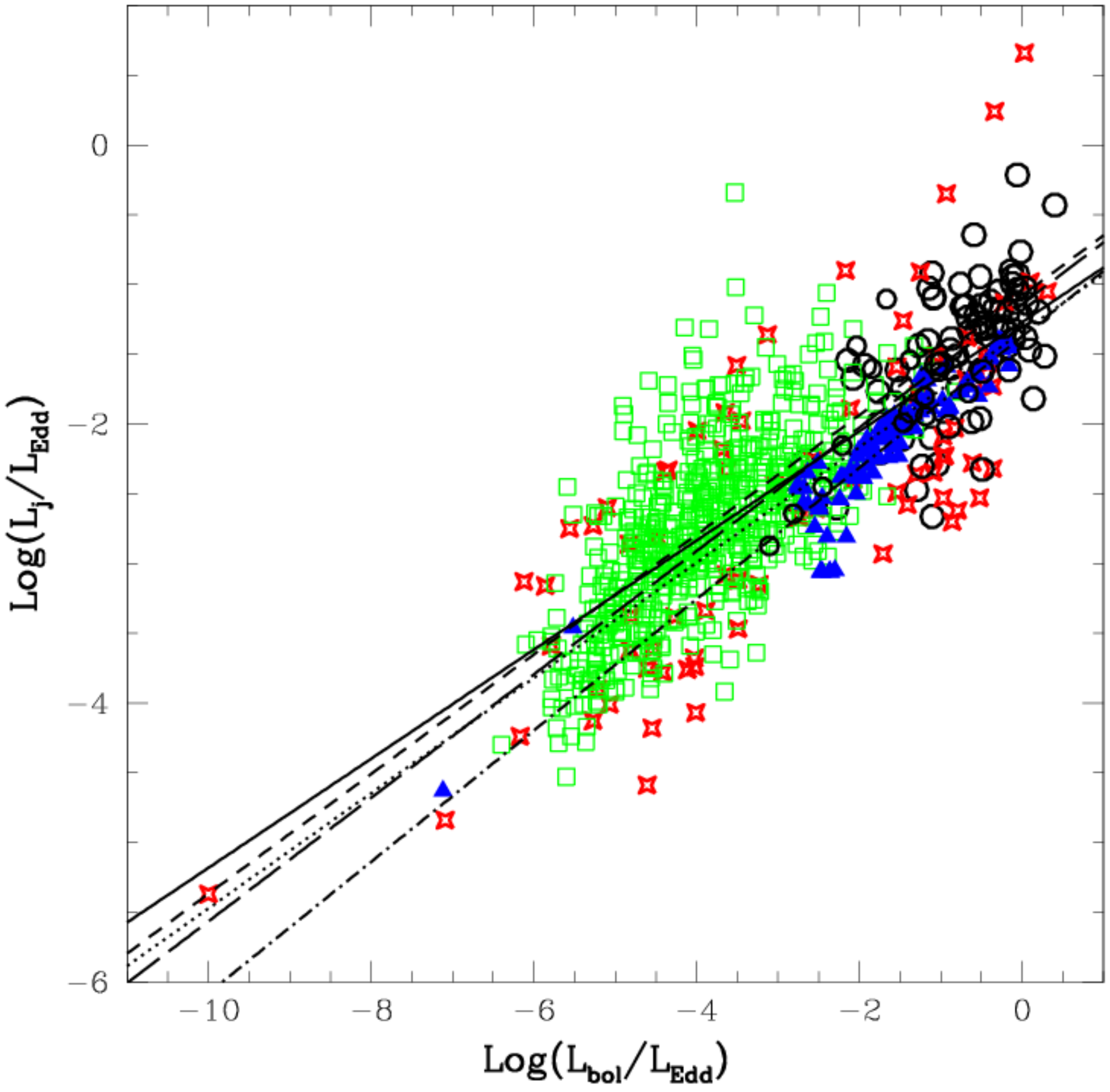

4 Categories of BH considered (D+18):

3 types of supermassive BH +
1 type of stellar-mass BH

100 FRII sources - shown in black (D16)
576 LINERs (Nisbet & Best 2016) – shown in green
80 AGN (Merloni et al. 2003) – shown in red
102 Stellar-mass Galactic black holes – shown in blue (Saikia et al. 2015)

Best fit slopes A:

0.44 ± 0.05	**for 100 FRII sources (long-dashed line)**
0.43 ± 0.02	**for 576 LINERs (med-dashed line)**
0.41 ± 0.04	**for 80 Compact RS AGN (dotted line)**
0.47 ± 0.02	**for 102 GBH (dot-dashed line)**

The solid line shows the fit to all sources (from D+18)

=> $(L_j/L_{Edd}) \propto (L_{bol}/L_{EDD})^A$ Strictly empirical

Empirically studies of L_j , L_{bol} , L_{EDD} indicate:

$$(L_j/L_{Edd}) \propto (L_{bol}/L_{EDD})^A$$ (empirical relationship D16, D+18)

Theoretical expectation for spin powered outflow models (e.g. Blandford & Znajek 1977; Meier 1999), is $L_j \propto B_p^2 L_{Edd}^2 F^2$. This can be re-written in dimensionless, separable form (D19):

$$(L_j / L_{Edd}) = g_j (B/B_{Edd})^2 F^2$$ Theoretical Eq. for spin powered outflow model in DSF

B = disk field strength; $(B_p/B)^2$ is absorbed into g_j; & $B^2_{Edd} \propto M^{-1} \propto (L_{EDD})^{-1}$ (e.g. Rees 1984)

B_p => poloidal component of B field - anchored in accretion disk and threading the BH region

=> $$(B/B_{Edd})^2 = (L_{bol}/L_{EDD})^A$$ (D19, D21)

⇒ $$B = B_{Edd} (L_{bol}/L_{EDD})^{A/2}$$ since $B^2_{Edd} \propto M^{-1} \propto (L_{EDD})^{-1}$ (e.g. Rees 1984)

=> $$F^2 = f(j)/f_{max} = (L_j / g_j L_{Edd}) (L_{bol} / g_b L_{Edd})^{-A}$$ (D16,D19)

where $F = (f(j)/f_{max})^{1/2} = j/[1+ (1 – j^2)^{1/2}]$ **[requires $j \leq 1$, so empirical values of $F > 1$ => $j = 1$]**

j => dimensionless black hole spin, sometimes denoted a_* or a in other work

With L_j and L_{bol} normalized by L_j (max) = $g_j L_{EDD}$ and L_{bol} (max) = $g_b L_{EDD}$

Results shown indicate $g_j = 0.1$ and $g_b = 1$; take these throughout (see empirical results of D+18)

576 LINERS (NB16) 80 Local AGN (M03) 100 FRII AGN (D16/D19) 102 measurements of 4 GBH (S15)

Adopting $g_j \cong 0.1$, $g_b \cong 1$ for all source types. $\delta(\mathrm{LogF}) \cong 0.07, 0.15, 0.15, 0.19$ (GBH, FRII, LINERs, M03)

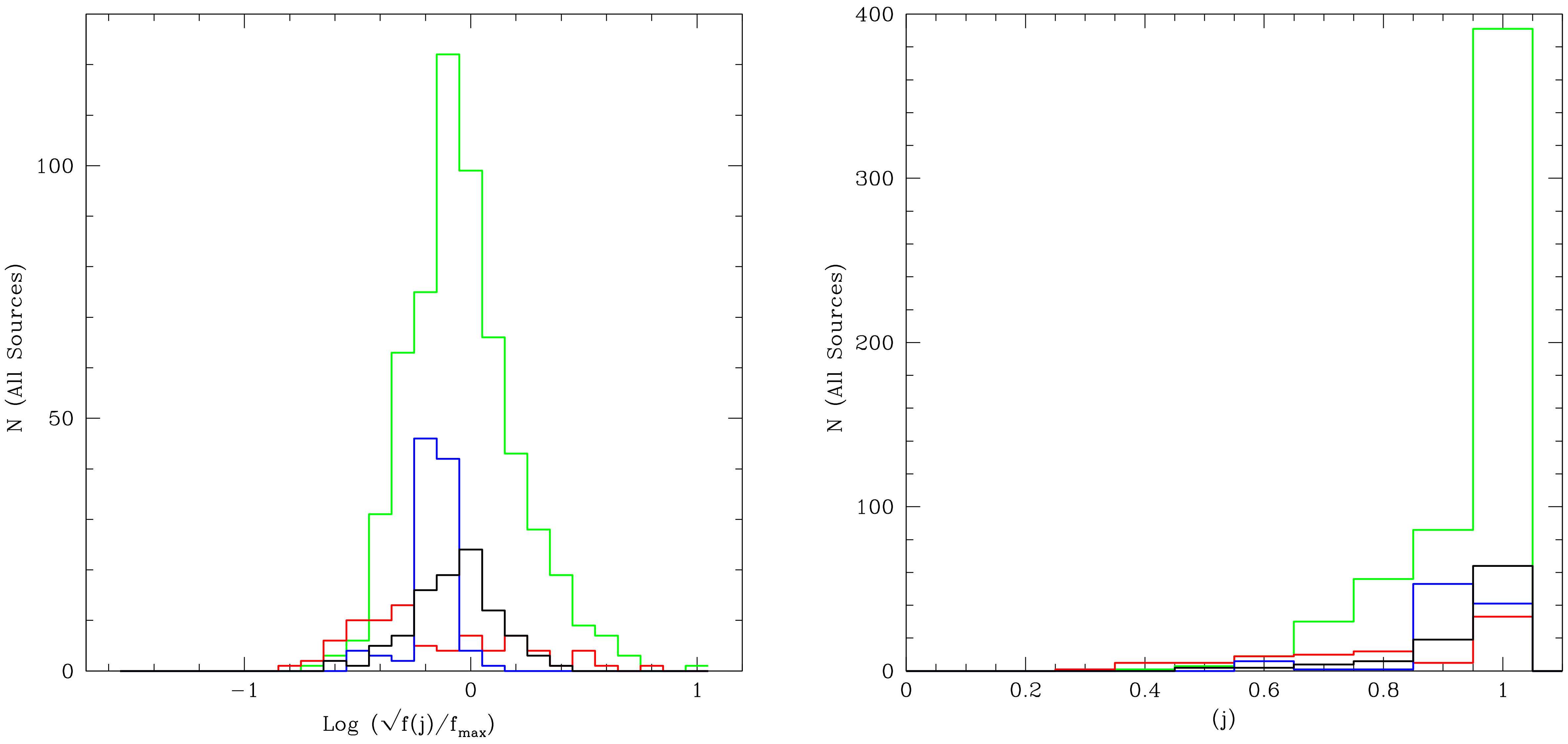

LINERs
FRII RS
Compact RS
X-R-Binaries

Table 1. Mean Value and Standard Deviation of Histograms and Values for Select Individual Sources. [a]

(1) Sample	(2) Type	(3) N [b]	(4) $\text{Log}\sqrt{(f(j)/f_{max})}$	(5) j	(6) j_{pub} (ref)[c]	(7) Log(B/B$_{Edd}$)	(8) Log(B/10^{4}G)
NB16(1)[d]	AGN	576	$-0.04 \pm 0.24(0.14)$	0.93 ± 0.10		$-0.83 \pm 0.21(0.10)$	$-0.09 \pm 0.39(0.22)$
D16	AGN	97	$-0.07 \pm 0.19(0.15)$	0.93 ± 0.11		$-0.19 \pm 0.17(0.12)$	$0.03 \pm 0.23(0.23)$
M03	AGN	80	$-0.17 \pm 0.36(0.19)$	0.81 ± 0.20		$-0.58 \pm 0.42(0.13)$	$0.27 \pm 0.66(0.37)$
S15	GBH	102	$-0.17 \pm 0.10(0.07)$	0.92 ± 0.09		$-0.37 \pm 0.23(0.06)$	$4.00 \pm 0.24(0.06)$
GX 339-4	GBH	76	-0.17 ± 0.06	0.92 ± 0.06	0.94 ± 0.02 (1)	-0.32 ± 0.18	4.07 ± 0.18
GX 339-4					$0.95^{+0.03}_{-0.05}$ (2)		
V404 Cyg	GBH	20	-0.10 ± 0.06	0.97 ± 0.02		-0.44 ± 0.24	3.84 ± 0.24
XTE J1118 [e]	GBH	5	-0.43 ± 0.01	0.66 ± 0.02		-0.54 ± 0.01	3.80 ± 0.01
AO6200 [f]	GBH	1	-0.08 ± 0.07	0.98 ± 0.07		-1.62 ± 0.06	2.76 ± 0.06
Sgr A^*	AGN	1	-0.17 ± 0.19	0.93 ± 0.15		-2.09 ± 0.13	-0.61 ± 0.37
M87 [g]	AGN	1	0.13 ± 0.19	1.00 ± 0.15		-1.19 ± 0.13	-1.16 ± 0.37
Ark 564	AGN	1	0.06 ± 0.19	1.00 ± 0.15	$0.96^{+0.01}_{-0.11}$ (3)	0.17 ± 0.13	1.93 ± 0.37
Mrk 335	AGN	1	-0.29 ± 0.19	0.81 ± 0.15	> 0.91 (3)	-0.15 ± 0.13	1.06 ± 0.37
Mrk 335					$0.70^{+0.12}_{-0.01}$ (4)		
Mrk 335					$0.83^{+0.10}_{-0.13}$ (5)		
NGC 1365	AGN	1	0.53 ± 0.19	1.00 ± 0.15	> 0.84 (3)	-0.64 ± 0.13	0.70 ± 0.37
NGC 4051	AGN	1	-0.02 ± 0.19	1.00 ± 0.15	> 0.99 (3)	-0.34 ± 0.13	1.30 ± 0.37
NGC 4151	AGN	1	-0.27 ± 0.19	0.84 ± 0.15	> 0.9 (3)	-0.35 ± 0.13	0.60 ± 0.37
3C 120	AGN	1	0.59 ± 0.19	1.00 ± 0.15	> 0.95 (3)	-0.13 ± 0.13	0.78 ± 0.37

[a]Obtained for $g_{bol} = 1$ and $g_j = 0.1$ for all sources. The estimated uncertainty per source is included in brackets following the standard deviation in columns (4), (7), and (8) for the samples listed in the top part of the table, as discussed in section 3.3. The bottom part of the table includes entries for three individual GBH, which have multiple observations per source, one additional GBH, and several individual AGN.

[b]N is the number of sources for the AGN and the number of measurements for the GBH.

[c]Published spin values; the citations are: (1) Miller et al. (2009); (2) Garcia et al. 2015; (3) Vasudevan et al. (2016); (4) Patrick et al. (2012); and (5) Walton et al. (2013).

Key Results Obtained with the Outflow Method

I). Black hole spin is unrelated to source type for the 4 categories of BH systems studied:
Spins are similar for GBH, LINERS, local AGN (S&L), & classical double (FRII) sources => HEG, LEG, & Quasars

II). Spins are relatively high: the M03 sample, which includes many nearby lower luminosity AGN, includes sources with lower spin, $j \cong (0.4 - 1)$ (preponderance of high values may be due to selection effects)

III). Method and results are empirically based => independent of any specific accretion disk model, & independent of a specific jet model relating outflow beam power to radio emission.
Thus, the results can be used to study and constrain accretion disk and jet formation models.

IV). There are three empirical indications that the outflows are powered by the BH Spin:

1). Accretion disk B field strengths obtained with the outflow method **agree** with those obtained in the context of specific accretion disk models (that do not consider source outflow properties) (AGN & stellar-mass BH [GBH])

2). Mass accretion rates and disk radiant efficiency factors obtained with the outflow method **agree** with those obtained in the context of specific accretion disk models (that do not consider outflow properties)

3). There are numerous sources with $L_j \approx (10 - 100)\ L_{bol}$ (Hard to understand without spin powered outflows)